Advances in Science and Technology Research Journal

Advances in Science and Technology Research Journal 2022, 16(5), 100–109
https://doi.org/10.12913/22998624/153965
ISSN 2299-8624, License CC-BY 4.0

Received: 2022.06.29
Accepted: 2022.10.17
Published: 2022.11.01

Experimental Research on the Influence of the Composition of the Fuel Mixture on the Operating Parameters of a Single-Cylinder Common Rail Diesel Engine

Karol Tucki[1*], Remigiusz Mruk[1]

[1] Institute of Mechanical Engineering, Department of Production Engineering, Warsaw University of Life Sciences, ul. Nowoursynowska 164, 02-787 Warsaw, Poland

* Corresponding author's e-mail: karol_tucki@sggw.edu.pl

ABSTRACT

The article presents the laboratory tests results of the influence of the diesel oil content in a mixture with rapeseed oil on the operating parameters of a diesel engine with the common rail fuel supply system. Fuel mixtures with a rapeseed content of 0, 50, 70, 100% were used. The article presents the results of tests carried out for various configurations of the object. The measurements included tests of exhaust gases: the content of carbon monoxide, carbon dioxide, hydrocarbons, nitrogen oxides as well as specific fuel consumption and exhaust gas temperature. As a result of the research, it was noticed that the use of rapeseed oil causes a significant increase in fuel consumption and an increase in emissions. At a crankshaft speed of 2500 rpm and a torque generated by the engine crankshaft of 12 Nm, the specific fuel consumption for a 0% rapeseed content is 310 g/kWh. For the same engine operating conditions and the same rapeseed content of the fuel, the fuel consumption for 100% rapeseed content is 330 g/kWh. For the same engine operating parameters, analysis of the carbon dioxide content in the exhaust gas yields a value of 7.8×10^4 ppm for a rapeseed content of 0%. For the same engine operating conditions and for the oilseed rape content in the fuel is 100% 8.4×10^4 ppm. The mathematical models describing the effects of engine operating parameters and rapeseed oil content in the mixture on the observed values were created with the Scilab program. The degree of agreement of the determined mathematical models was checked by calculating the coefficient of determination (R2). The results are shown in 3D figures.

Keywords: vehicle, biofuel, fuel, common rail.

INTRODUCTION

One of the European Union's priorities is to reduce greenhouse gas emissions [1]. Road transport is the largest source of greenhouse gas emissions in the European Union [2]. More and more restrictive legal regulations are being introduced [3]. In 2020, the average carbon dioxide emissions for vehicles sold by individual brands must have been below 120 g/km. As of January 1, 2021, this limit has been lowered to 95 g/km. The reduction in average CO_2 emissions of 95 g/km is the strictest in the world [4]. For comparison – in 2021 this limit in the United States was 125 g/km, in Japan it was 122 g/km and in China it was 117 g/km [5].

In July 2021, the European Commission adopted a package of legislative proposals called "Fit for 55" as part of the European Green Deal, which aims to strengthen the EU's position as a global climate leader [6]. The most important assumptions of the new regulations include the revision of the directive on alternative fuels infrastructure as well as the amendment of the existing regulation that sets CO_2 emission standards for passenger cars and vans [7]. The new regulations introduce a requirement to reduce average emissions from brand new cars by 55%. from 2030 and by 100% five years later [8]. This means that it will not be possible to sell new cars with internal combustion engines in the EU from 2035 [9].

Therefore, automotive companies are forced to use more and more advanced technologies [10]. The elements that are being introduced include: more efficient and less fuel-consuming combustion engines [11], alternative methods of powering vehicles (electric cells, fuel cells) as well as alternative fuels and biofuels, such as ethers, esters, alcohols or hydrocarbon fractions obtained from biomass [12].

The growing interest in new fuel components results from several factors [13]. The first is, of course, environmental considerations [14]. No less important are the economic conditions: an increase in the prices of crude oil and natural gas and the depletion of their existing deposits [15]. Certain political factors are of importance as well: dependence on the supply of raw materials from abroad as well as the requirement to reduce greenhouse gas emissions to the atmosphere, which results from international agreements [16].

The use of ever increasing amounts of bio-based fuels in diesel engines leads to changes in the combustion process in the engine chambers, due to their different characteristics [17, 18].

The available literature lacks sufficient objective information about the influence of biofuels on injection systems [19] and combustion processes [20]. The experimental tests will make it possible to determine the phenomena that occur during the combustion process when the type of fuel is changed, and may help to optimize the engine parameters. The basic research on combustion processes can provide knowledge on how to modify operational diesel engines for the use of biofuels [21].

The research presented in the paper was carried out on a stand with a single-cylinder engine, with the possibility of modifying various factors that affect the combustion process.

New at work is the use of the common rail system for a single-cylinder engine with a power output of 5.7 kW.

MATERIALS AND METHOD

The aim of the paper and the extent of research

The aim of the research was to measure the operating parameters of a Farymann 18W compression-ignition engine powered by various types of fuels.

The scope of the research included the following types of fuels:

- diesel fuel (100% diesel);
- rapeseed oil (100% oil);
- a mixture of rapeseed oil and diesel oil (70% oil + 30% diesel);
- a mixture of rapeseed oil and diesel fuel (50% oil + 50 % diesel).

The scope of the research included changes in the following parameters:

- rotational speed: 2000, 2500 rpm;
- torque: 2–12 Nm.

The measured and determined engine parameters – exhaust gas concentration:

- carbon monoxide content ppm (CO);
- carbon dioxide content ppm (CO_2);
- hydrocarbon content ppm (HC);
- content of nitrogen oxides ppm (NO_x).

Measurements on the stand:

- unit fuel consumption g/kWh (g_e);
- exhaust gas temperature °C (T_s).

Test stand

The test stand was built on the basis of the Farymann serial production diesel engine – type 18 W Marine "Yellow River Star" (FD18WM) [22]. It is a four-stroke, compression-ignition, naturally aspirated, direct injection engine [23]. The engine has one vertically positioned cylinder with a displacement of 290 cm^3. The cylinder diameter is $\varnothing d$ = 82 mm, the piston stroke is s = 55 mm. The result is the ratio of the piston stroke to the cylinder diameter s/d = 0.6875. The chamber capacity in the piston is VK = 10.6 cm^3, the compression ratio is ε = 20. Figure 1 shows the test engine and its basic parameters.

In order to ensure the correct interaction of individual elements of the test stand, i.e. the engine, power supply system, exhaust gas system, cooling system as well as the clutch, electrical brake and control-measurement system, these components were placed in a specially constructed frame.

The fuel supply system was modified and parts of the original mechanical injection system were removed and replaced with the CommonRail (CR) electronic fuel injection system. The CR system consists of a fuel intake section, a replaceable in-line filter, a low pressure pump, a temperature stabilizer, a high pressure CR fuel pump, a receptacle – a pressure accumulator known as the Rail, and a CR injector. Figure 2

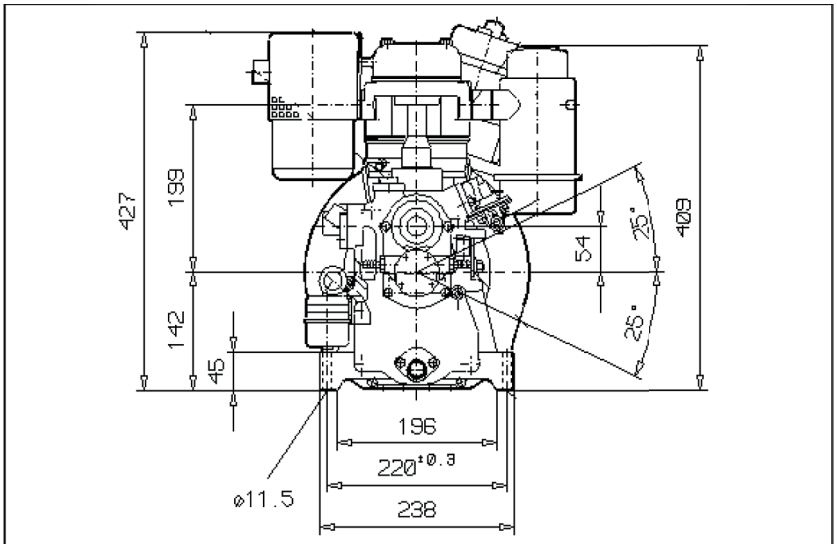

Model			18W
Cylinder position			upright
Number of cylinders			1
Diameter Stroke		mm mm	82 55
Displacement		cm^3	290
Oil usage		g/kWh	1
Amount of oil		l	1
Max. Power (3600 min^{-1})	(3000 min^{-1}) IFN-ISO ICFN-ISO	kW (PS) kW (PS) kW (PS)	5.70 (7.75) 5.20 (7.07) 4.70 (6.39)
Average piston speed at maximum rotational speed		m/s	6.6 / 3600
Compression ratio			20:1
Fuel tank capacity		l	4
Max rotational speed Max torque		min^{-1} Nm (min^{-1})	3600 16.7 (2400)
Weight excluding fluids		kg	37
Water demand with direct cooling		l/min	7-8

Fig. 1. Diagram and main dimensions of the Farymann 18W engine

presents an 18W motor installed on the test stand and elements of the power supply system.

The fuel intake section was positioned in such a way as to conveniently change the type of fuel supplied and to enable the measurement of its consumption. For this purpose, a stand was constructed and equipped with replaceable receptacles and an electronic scales for measuring the amount of fuel consumed.

The exhaust gas system consisted of an exhaust manifold, a bellows compensator (installed to compensate for vibrations) and two mufflers arranged in series. There are gas-tight gates in the exhaust system for the installation of a thermocouple for measuring exhaust gas temperature, probe tips for measuring the chemical composition of exhaust gases and a probe for measuring exhaust opacity. The exhaust system is connected to a chimney system with a high temperature resistant rubber conduit that carries exhaust gases outside the building.

Measurement devices

The tests were carried out on a measuring stand equipped with:

- three-phase synchronous generator type ECO 28-1L/2 from Mecc Alte for torque loading of the engine to be tested. It is a brushless synchronous three-phase current generator in which the braking torque is regulated by changing the excitation current;
- 2000 Series Torque Meter from NTCE AG for measuring the engine torque and the crankshaft speed of the engine;

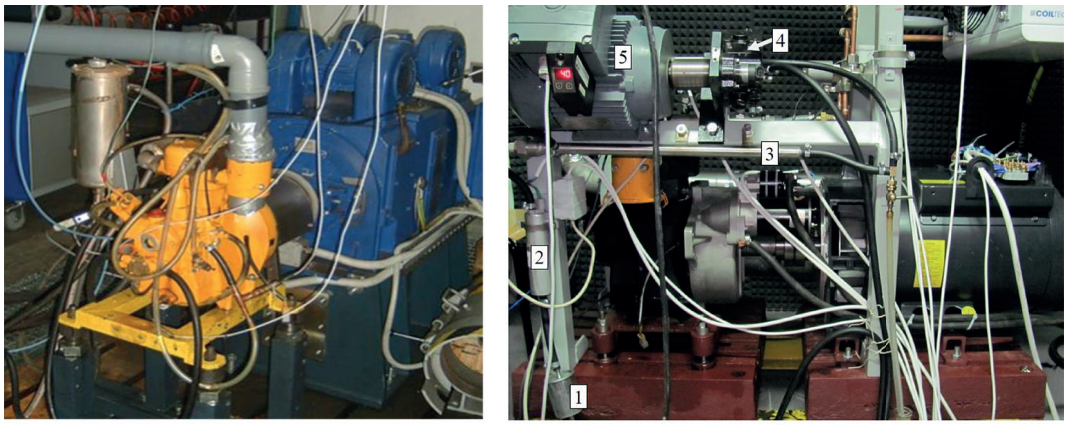

a b

Fig. 2. Test stand: a – an 18W engine installed on the test stand; b – elements of the supply system: 1 – fuel filter, 2 – low pressure pump, 3 – temperature stabilizer, 4 – high pressure CR pump, 5 – CR pump drive motor

- scales Radwag WLC 20/A2 for measuring the mass of fuel consumption by the engine;
- mass Flowmeter from Sierra Instruments Inc. Type 620S Fast-Flo for measuring the air mass delivered to the engine;
- multifunction exhaust gas analyzer GA-40 T plus MADUR for measuring exhaust gas components;
- PC with M-Series multifunctional PCI cards and National Instruments' LABVIEW software for controlling and recording test results.

Fuels

Table 1 presents the physicochemical parameters of the fuels used in the tests [24, 25].

RESEARCH RESULTS

The experimental tests of the engine were carried out for various engine operating parameters and different fuel mixture compositions. The example results of the conducted experiments are presented below. Each of the experimental points in the graphs below equals the mean of the values obtained during the test. The way in which the experimental studies are carried out corresponds to the research methodology of other authors [26].

Exhaust gas tests

Figure 3 shows the change in the CO (carbon monoxide) content as a function of the

Tabela 1. Basic properties of fuels used in tests

Properties	Diesel	Rapeseed oil
Density kg/dm^3 (15°C)	0.817–0.856	0.91–0.92
Kinetic viscosity (mm^2/sec) (20°C)	2.90–5.50	68–97.7
Calorific value MJ/kg	42.7–43.5	36.7–37.7
Calorific value MJ/dm^3	35.69–35.75	33.7–34.04
Cetane number LC	47.10–58.60	40–44
Molar mass kg/kmol	120–320	882–883
Stoichiometric oxygen demand kg_{air}/kg_{fuel}	14.57	12.43
Elemental analysis		
C (%)	86.0–86.4	77.0–78.0
H (%)	13.4 0 14.0	10.0–11.7
O (%)	-	10.5–12.0
CFPP (°C)	+2 - 35	+5….+18
Condradson number (M%)	0.01–0.04	<0.01–0.5
Sulphur content (%)	0.03–0.22	0.009–0.012
Ignition temperature (°C)	20–84	317–324
Content of aromatic compounds (%)	21.5	-

composition of the fuel mixture as well as torque and rotational speed.

At a crankshaft speed of 2500 rpm and a torque generated by the engine crankshaft of 12 Nm, CO content in the exhaust gas for the oilseed rape content in the fuel 0% is 2250 ppm. For the same engine operating conditions and the oilseed rape content 100% 3400ppm. The results of the study also confirm scientific observations of other authors [27].

Figure 4 shows the change in the CO_2 (carbon dioxide) content as a function of the composition of the fuel mixture as well as torque and rotational speed.

At a crankshaft speed of 2500 rpm and a torque generated by the engine crankshaft of 12 Nm, the CO_2 content in the exhaust gas for the oilseed rape content in the fuel 0% is 7.8×10^4ppm. For the same engine operating conditions and oilseed rape content 70% 8.2×10^4ppm.

Figure 5 shows the change in the HC content (hydrocarbons) as a function of the composition of the fuel mixture as well as torque and rotational speed.

At a crankshaft speed of 2500 rpm and a torque generated by the engine crankshaft of 12 Nm, an HC content in the exhaust gas is obtained for the oilseed rape content in the fuel 0% is 320 ppm. For the same engine operating conditions and oilseed rape content 100% 1200 ppm.

The change in the NO_x (nitrogen oxides) content as a function of the fuel mixture composition as well as torque and rotational speed is shown in Figure 6.

At a crankshaft speed of 2500 rpm and a torque generated by the engine crankshaft of 12 Nm, a NO_x content in the exhaust gas was reached for the oilseed rape content in the fuel is 680 ppm. For the same engine operating conditions and oilseed rape content 100% was 670ppm.

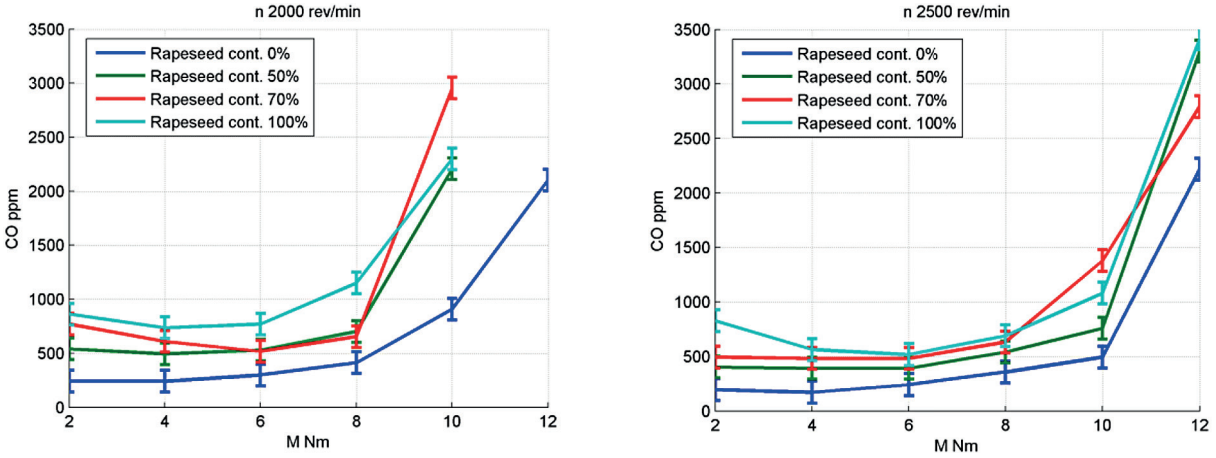

Fig. 3. Carbon monoxide content ppm (CO): M – torque Nm; n – rotational speed rpm; CO – CO content ppm

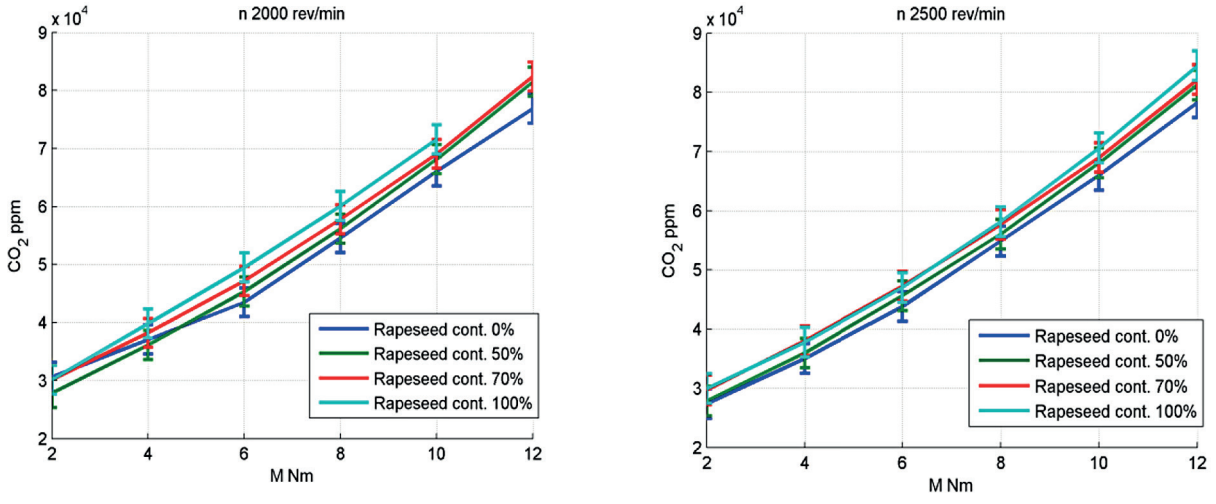

Fig. 4. Carbon dioxide content ppm (CO_2): M – torque Nm; n – rotational speed rpm; CO_2 – CO_2 content ppm

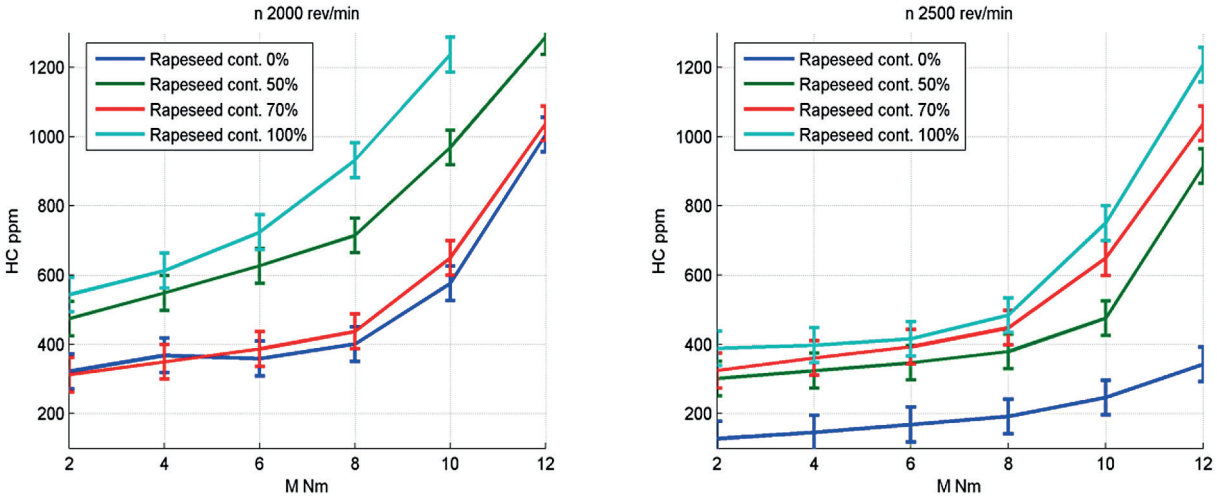

Fig. 5. Hydrocarbon content ppm (HC): M – torque Nm; n – rotational speed rpm; HC – HC content ppm

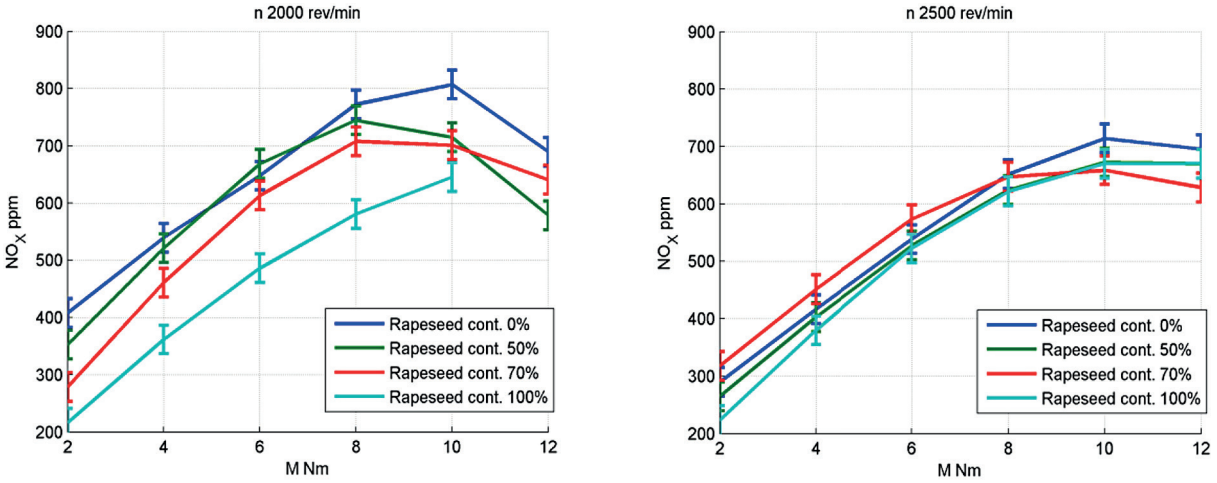

Fig. 6. Nitrogen oxides content ppm (NO_x): M – torque Nm; n – rotational speed rpm; NO_x – NO_x content ppm

Scientific studies by the authors of the article [28] have shown that NO_x emissions are reduced when the engine is run on rapeseed oil compared to diesel fuel.

The change in specific fuel consumption is shown in Figure 7. At a crankshaft speed of 2500 rpm and a torque generated by the engine crankshaft of 12 Nm, the specific fuel consumption for the oilseed rape content in the fuel is 310 g/kWh. For the same engine operating conditions and oilseed rape content 100% was 340 g/kWh.

Figure 8 shows the change in exhaust gas temperature as a function of the fuel mixture composition as well as torque and rotational speed.

At a crankshaft speed of 2500 rpm and a torque generated by the engine crankshaft of 12 Nm, an exhaust gas temperature for the oilseed rape content in the fuel is 0% was reached 285 °C. For the same engine operating conditions and the oilseed rape content 100% was 310 °C.

Table 2 presents the summary of the results of the estimation of partial correlation coefficients that determine the influence of independent variables on the observed values.

In the prepared experiment, fuel mixtures with a rapeseed content of 0, 50, 70, 100% were used. Table 2 shows the values of the partial correlation coefficients used to determine the effect of the individual independent variables (torque, speed, rapeseed content) on the individual observed values. These are dimensionless values in the range 0–1.

The numerical nonlinear regression tool (datafit function) included in the Scilab package was used to create mathematical models to describe the effects of engine operating parameters (crankshaft speed, crankshaft torque) and the rapeseed oil content of the mixture on the observed values (CO, CO_2, HC, NO_x, g_e, T_s).

The degree of agreement of the resulting mathematical models was checked by calculating the

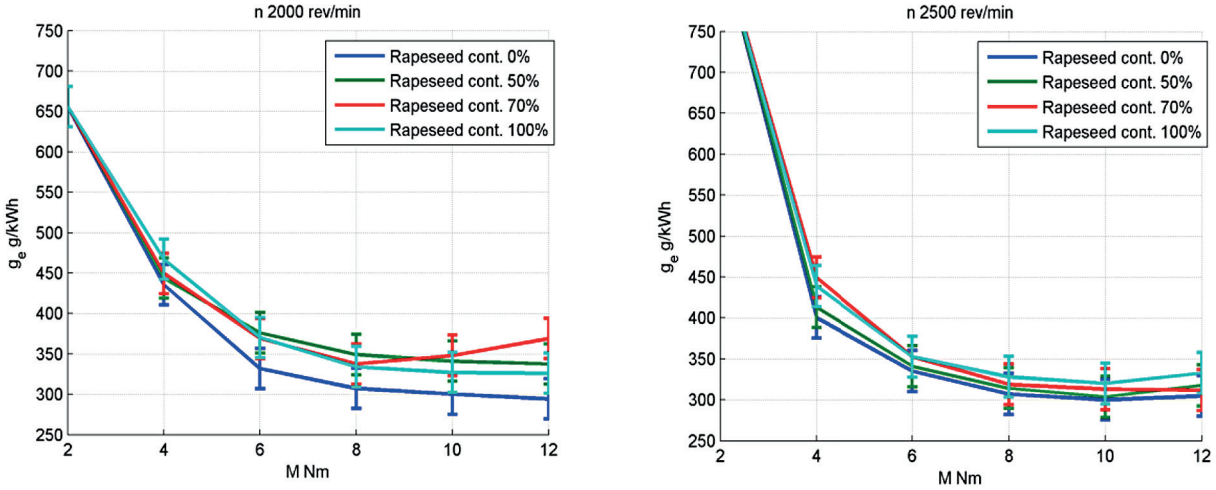

Fig. 7. Change of specific fuel consumption g/kWh (g_e): M – torque Nm; n – rotational speed rpm; g_e – specific fuel consumption g/kWh

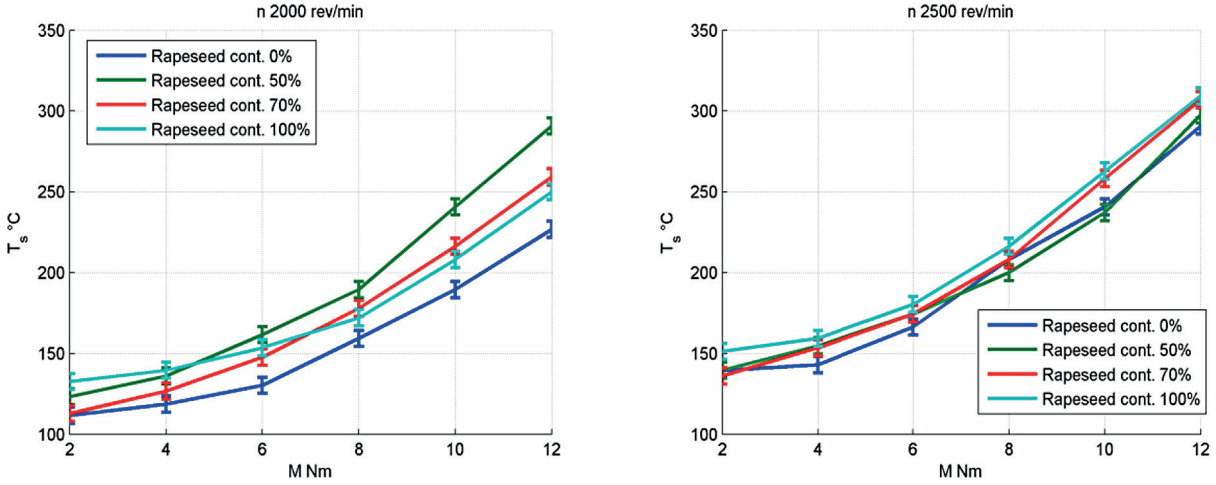

Fig. 8. Change of exhaust gas temperature g/kWh (T_s): M – torque Nm; n – rotational speed rpm; T_s – exhaust gas temperature °C

coefficient of determination R^2 (coefficient of determination) according to the following dependencies:

$$R^2 = \frac{\sum_{i=1}^{n}(y_{mi} - \overline{y})^2}{\sum_{i=1}^{n}(y_i - \overline{y})^2} \quad (1)$$

where: y_i – i-th observation of variables *y*;
y_{mi} – theoretical value of the explained variable (based on the model);
$\overline{y}$ – arithmetic mean of the empirical values of the explained variables (based on model).

A summary of the results of fitting the applied quantitative models is presented in Table 3 – M – torque Nm; N – rotational speed rpm; R – rape content %.

Figure 9 shows the image of the mathematical model of CO and CO_2 content change – M

Tab. 2. The summary of the results of the estimation of partial correlation coefficients that determine the influence of independent variables on the observed values

Variable	Partial corr. of CO	Partial corr. of CO_2	Partial corr. of HC	Partial corr. of NO_x	Partial corr. of g_e	Partial corr. of T_s
Torque M, Nm	0.7021	0.9915	0.6561	0.7020	-0.7650	0.9123
Rape Content R, %	0.2286	0.0413	0.3883	-0.1017	0.0765	0.1096
Rotational Speed n, rev/min	-0.0010	0.0239	-0.3302	-0.1831	0.0367	0.2744

Table 3. The results of fitting the applied quantitative models

Parameter	Model	R^2
CO	CO = *b*1**M*^2 + *b*2**M* + *b*3**R*^2 + *b*4**R* + *b*5	0.8295
CO_2	CO2 = *b*1**M*^2 + *b*2**M* + *b*3**R*^2 + *b*4**R* + *b*5	0.9971
HC	HC = *b*1**M*^2 + *b*2**M* + *b*3**R*^2 + *b*4**R* + *b*5**n* + *b*6;	0.8248
NO_x	NOX = *b*1**M*^2 + *b*2**M* + *b*3**R*^2 + *b*4**R* + *b*5**n* + *b*6;	0.5583
g_e	ge = *b*1**M*^2 + *b*2**M* + *b*3**R*^2 + *b*4**R* + *b*5	0.8709
T_s	Ts = *b*1**M*^2 + *b*2**M* + *b*3**R*^2 + *b*4**R* + *b*5**n* + *b*6;	0.9675

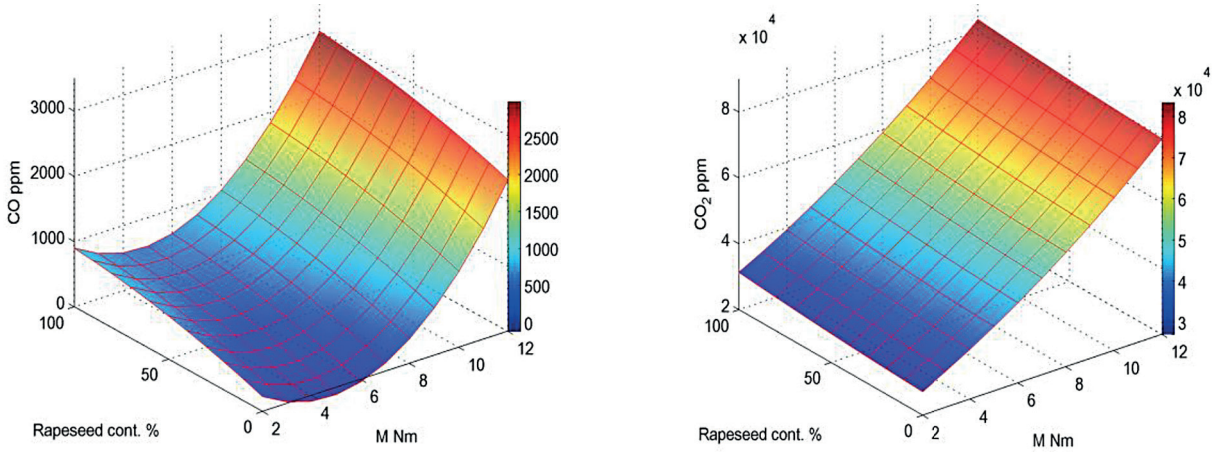

Fig. 9. Image of the mathematical model of CO and CO2 content change

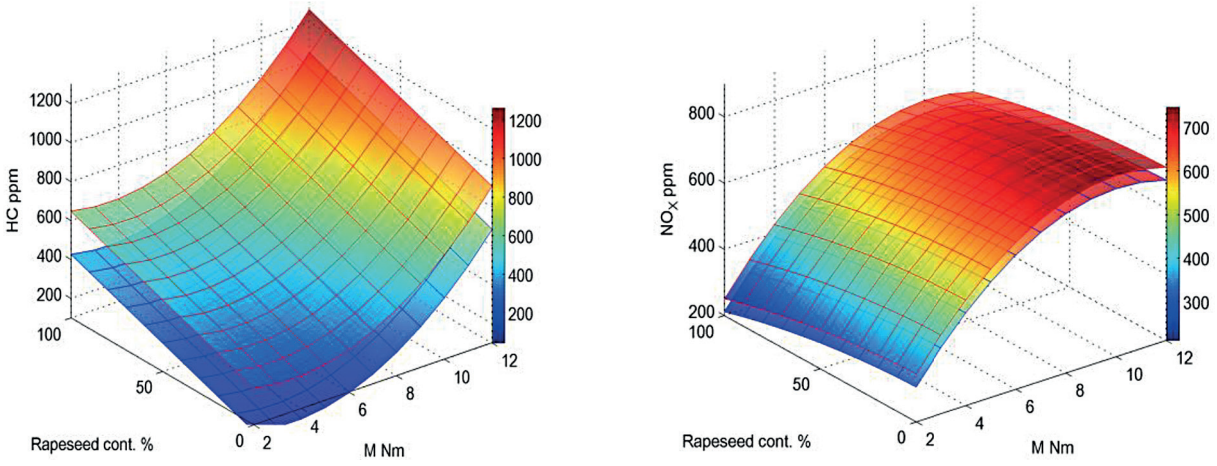

Fig. 10. Picture of the mathematical model of HC and NO_X content change

– torque Nm; CO – carbon monoxide content ppm; CO_2 – carbon dioxide content ppm.

Figure 10 shows the image of the mathematical model of the change in HC and NO_X content – M – torque Nm; HC – hydrocarbons content ppm; NO_X – nitrogen oxides content ppm; n – rotational speed: 2000 rpm, 2500 rpm.

Figure 11 shows the image of the mathematical model of the change g_e i T_s – M – torque Nm; g_e – specific fuel consumption g/kWh; T_s – exhaust gas temperature °C; n– rotational speed: 2000 rpm, 2500 rpm.

The speeds used (2000 rev/min, 2500 rev/min) result from the position of the maximum torque of the engine (2400 rev/min, 16.7 Nm). The use of a maximum torque of 12 Nm in the tests resulted from the limitation of the maximum permissible smoke level.

CONCLUSIONS

On the basis of the conducted research, it can be concluded that the use of rapeseed oil increases

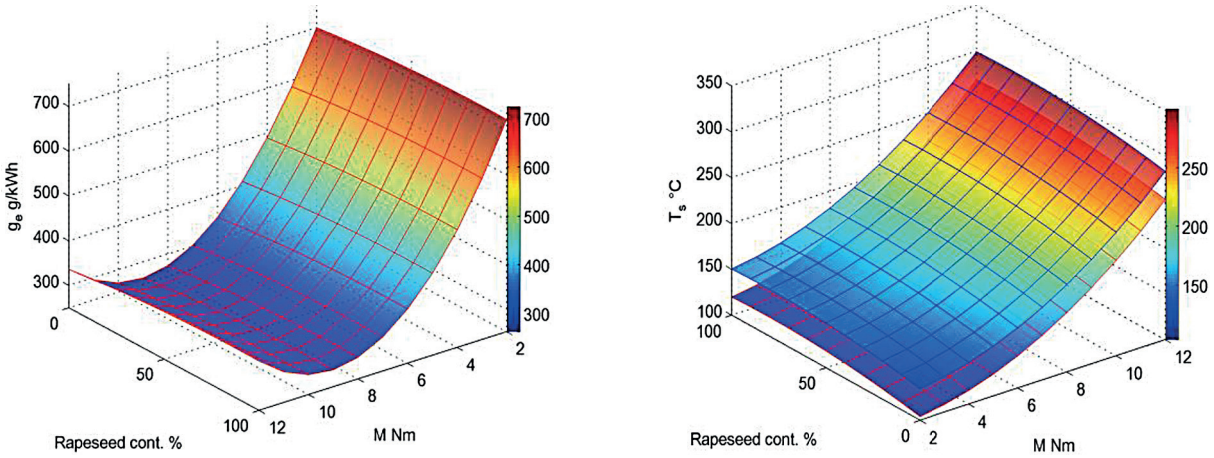

Fig. 11. The image of the mathematical model of the change of the contents of g_e and T_s

the opacity of exhaust gases. In order to maintain the same exhaust opacity value under the rated conditions as in the case of diesel fuel, the engine power should be reduced by approx. 3%. The use of rapeseed oil increases the fuel consumption of the engine by 6 to 13%. The use of diesel fuel with the addition of rapeseed oil causes an increase in CO, CO_2, THC emissions and a decrease in NO_X emissions. The characteristics of the engine powered by fuels with 70% and 50% rapeseed oil additions are in between those obtained for diesel oil and pure rapeseed oil. It appears advisable to modify the combustion chamber in such a way that the incineration process of rapeseed oil is carried out correctly. It appears advisable to conduct research on optimization of the injection advance angle for rapeseed fuels. It should also be noted that the calorific value of rapeseed oil is about 10% lower than that of ON. This results in a reduction in the engine power with the same fuel quantities.

REFERENCES

1. Nieuwenhuijsen M.J. Urban and transport planning pathways to carbon neutral, liveable and healthy cities; A review of the current evidence. Environment International. 2020; 140: 105661. https://doi.org/10.1016/j.envint.2020.105661
2. Puricelli S., Cardellini G., Casadei S., Faedo D., Van den Oever A.E.M., Grosso M. A review on biofuels for light-duty vehicles in Europe. Renewable and Sustainable Energy Reviews 2020; 137: 110398. https://doi.org/10.1016/j.rser.2020.110398
3. Tucki K., Orynycz O., Mitoraj-Wojtanek M. Perspectives for Mitigation of CO2 Emission due to Development of Electromobility in Several Countries. Energies. 2020; 13: 4127. https://doi.org/10.3390/en13164127
4. Anselma P.G. Electrified powertrain sizing for vehicle fleets of car makers considering total ownership costs and CO2 emission legislation scenarios. Applied Energy. 2022; 314: 118902. https://doi.org/10.1016/j.apenergy.2022.118902
5. Heinold A. Comparing emission estimation models for rail freight transportation. Transportation Research Part D: Transport and Environment. 2020; 86: 102468. https://doi.org/10.1016/j.trd.2020.102468
6. Ovaere M., Proost S. Cost-effective reduction of fossil energy use in the European transport sector: An assessment of the Fit for 55 Package. Energy Policy. 2022; 168: 113085. https://doi.org/10.1016/j.enpol.2022.113085
7. Skov I.R., Schneider N. Incentive structures for power-to-X and e-fuel pathways for transport in EU and member states. Energy Policy. 2022; 168: 113121. https://doi.org/10.1016/j.enpol.2022.113121
8. Tsiropoulos I., Siskos P., Capros P. The cost of recharging infrastructure for electric vehicles in the EU in a climate neutrality context: Factors influencing investments in 2030 and 2050. Applied Energy. 2022; 322: 119446. https://doi.org/10.1016/j.apenergy.2022.119446
9. Köhl M., Linser S., Prins K., Talarczyk A. The EU climate package "Fit for 55" – a double-edged sword for Europeans and their forests and timber industry. Forest Policy and Economics. 2021; 132: 102596. https://doi.org/10.1016/j.forpol.2021.102596
10. Papulová Z., Gažová A., Šufliarský L. Implementation of Automation Technologies of Industry 4.0 in Automotive Manufacturing Companies. Procedia Computer Science. 2022; 200: 1488–1497. https://doi.org/10.1016/j.procs.2022.01.350
11. Leach F., Kalghatgi G., Stone R., Miles P. The scope for improving the efficiency and environmental impact of internal combustion engines.

Transportation Engineering. 2020; 1: 100005. https://doi.org/10.1016/j.treng.2020.100005

12. Giampieri A., Ling-Chin J., Ma Z., Smallbone A., Roskilly A.P. A review of the current automotive manufacturing practice from an energy perspective. Applied Energy. 2020; 261: 114074. https://doi.org/10.1016/j.apenergy.2019.114074
13. Gao J., Chen H., Li Y., Chen J., Zhang Y., Dave K., Huang Y. Fuel consumption and exhaust emissions of diesel vehicles in worldwide harmonized light vehicles test cycles and their sensitivities to eco-driving factors. Energy Conversion and Management. 2019; 196: 605–613. https://doi.org/10.1016/j.enconman.2019.06.038
14. Cantillo V., Amaya J., Serrano I., Cantillo-García V., Galván J. Influencing factors of trucking companies willingness to shift to alternative fuel vehicles. Transportation Research Part E: Logistics and Transportation Review. 2022; 163: 102753. https://doi.org/10.1016/j.tre.2022.102753
15. Kim K., Lee J., Kim J. Can liquefied petroleum gas vehicles join the fleet of alternative fuel vehicles? Implications of transportation policy based on market forecast and environmental impact. Energy Policy. 2021; 154: 112311. https://doi.org/10.1016/j.enpol.2021.112311
16. Kluschke P., Gnann T., Plötz P., Wietschel M. Market diffusion of alternative fuels and powertrains in heavy-duty vehicles: A literature review. Energy Reports. 2019; 5: 1010–1024. https://doi.org/10.1016/j.egyr.2019.07.017
17. Wang Y., Hao C., Ge Y., Hao L., Tan J., Wang X., Zhang P., Wang Y., Tian W., Lin Z., Li J. Fuel consumption and emission performance from light-duty conventional/hybrid-electric vehicles over different cycles and real driving tests. Fuel; 2020; 278: 118340. https://doi.org/10.1016/j.fuel.2020.118340
18. Seum S., Ehrenberger S., Pregger T. Extended emission factors for future automotive propulsion in Germany considering fleet composition, new technologies and emissions from energy supplies. Atmospheric Environment. 2020; 233: 117568. https://doi.org/10.1016/j.atmosenv.2020.117568
19. Dhahad H.A., Fayad M.A., Chaichan M.T., Jaber A.A., Megaritis T. Influence of fuel injection timing strategies on performance, combustion, emissions and particulate matter characteristics fueled with rapeseed methyl ester in modern diesel engine. Fuel. 2021; 306: 121589. https://doi.org/10.1016/j.fuel.2021.121589
20. Zhang Z.E.J., Chen J., Zhao X., Zhang B., Deng Y., Peng Q., Yin Z. Effects of boiling heat transfer on the performance enhancement of a medium speed diesel engine fueled with diesel and rapeseed methyl ester. Applied Thermal Engineering. 2020; 169: 114984. https://doi.org/10.1016/j.applthermaleng.2020.114984
21. Kurczyński D., Łagowski P. Performance indices of a common rail-system CI engine powered by diesel oil and biofuel blends. Journal of the Energy Institute. 2019; 92: 1897–1913. https://doi.org/10.1016/j.joei.2018.11.004
22. Mohebbi M., Reyhanian M., Hosseini V., Said M.F.M., Aziz A.A. The effect of diethyl ether addition on performance and emission of a reactivity controlled compression ignition engine fueled with ethanol and diesel. Energy Conversion and Management. 2018; 174: 779–792. https://doi.org/10.1016/j.enconman.2018.08.091
23. Caligiuri C., Renzi M., Bietresato M., Baratieri M. Experimental investigation on the effects of bioethanol addition in diesel-biodiesel blends on emissions and performances of a micro-cogeneration system. Energy Conversion and Management. 2019; 185: 55–65. https://doi.org/10.1016/j.enconman.2019.01.097
24. Kordylewski W. Spalanie i Paliwa, 5th ed. Oficyna Wydawnicza Politechniki Wrocławskiej 2008.
25. Gwardiak H., Rozycki K., Ruszkarska M., Tylus J., Walisiewicz-Niedbalska W. Evaluation of fatty acid methyl esters (FAME) obtained from various feedstock. Rośliny Oleiste Oilseed Crop. 2011; 32: 137–147.
26. Naik B.D., Meivelu U., Thangarasu V., Annamalai S., Sivasankaralingam V. Experimental and empirical analysis of a diesel engine fuelled with ternary blends of diesel, waste cooking sunflower oil biodiesel and diethyl ether. Fuel. 2022; 320: 123961. https://doi.org/10.1016/j.fuel.2022.123961
27. Suchecki A., Nowakowski J. Operational aspects of fuel supply CI engine diesel oil with FAME. Autobusy: technika, eksploatacja, systemy transportowe. 2016; 6: 1148–1154.
28. Sander P., Longwic R., Lotko W., Niemczuk B. Current concepts of use of rapeseed oil as fuel. Autobusy: technika, eksploatacja, systemy transportowe. 2017; 18: 414–419.